



Study on Relationship of Residential Building Form Variations to Pollutant Dispersion in Streets

Jialei Shen¹, Zhi Gao^{1,*}, Wowo Ding¹, Wei You¹

¹ Nanjing University (NJU), Nanjing, China

*Corresponding email: zhgao@nju.edu.cn

SUMMARY

This paper investigates the influence of four representative residential building form variations to the street pollutant dispersion in the case of Nanjing. According to the quantitative analysis to the streets and residential buildings of Nanjing, the representative street structures, residential buildings and building form variations are present. The numerical results show that wind directions and building form variations have significant impacts on the pollutant dispersion. Appropriate building form variations are favourable to the pollutant dispersion for EW streets, while unfavourable for NS streets. Therefore, in order to facilitate the street ventilation, the prevailing wind directions and street orientations of the city should be taken into considerations in urban and building design. Besides, the annex buildings usually deteriorate the street ventilation.

KEYWORDS

Street morphology; Residential building; Street ventilation; Pollutant dispersion; CFD simulation

1 INTRODUCTION

Urbanization results in the ongoing expansion of urban areas and development of urban population, which is particularly common in the developing countries like China. The high-density compact urban areas generate great challenges to pollutant dispersion caused by vehicle emission, which is harmful to pedestrians' health. In recent years, vehicle emission has become one of the most significant air pollution sources in China's major cities.

A realistic urban area is of complex characteristics and it is difficult to fully study all details. Many previous studies mainly investigate urban canopy layer models with idealized geometries (Lin et al., 2014). Literatures have investigated the influence of urban morphology, street structure, ambient wind direction, packing densities and building height variability on urban ventilation and pollutant dispersion in idealized urban models (Hang et al., 2009, 2012, 2015; Di Sabatino et al., 2007; Salim et al., 2011; Ramponi et al., 2015; Hu and Yoshie, 2013).

In this paper, the representative street structures and residential building forms in China are summarized according to the quantitative analyses in the case of Nanjing. Four representative form variations of residential buildings along the streets are present by analyzing the typical street slices. This paper numerically investigates pollutant dispersion of different building

forms with CFD simulations, and aims to quantify the relationship of residential building form variations to pollutant dispersion in the streets, which is of great significance for urban design.

2 METHODS

Morphology characteristics analysis

The research area in this paper is the main city of Nanjing, including Old Town and Hexi New Town, which are typical areas with high-density residential buildings. The streets and residential buildings in Nanjing usually have uniform morphology characteristics. According to the statistical results of street morphology characteristics in Nanjing, the majority of the streets are less than 30m in width. The intersection distances of the streets are mainly in the range of 100m to 400m, among which 300m is commonest. The street orientations are mainly in east-west (EW) and north-south (NS), both more than 20% proportions.

Most of the residential buildings in Nanjing are slab forms. The commonest width of residential buildings is 12m. The building lengths are mainly in the range of 30m to 60m. Besides, the residential buildings are usually 6 stories. The majority of the residential buildings tend to be in NS orientation for better daylighting. Sparse urban configurations tend to obtain better urban ventilation, but have a low efficiency of land utilization, which is not suitable for the cities with high population densities like Nanjing. Therefore, the residential areas tend to have higher building density on the basis of meeting the requirements of the building interval distances regulated by national standard.

The residential buildings along the street are closely related to the pattern of street distribution. Figure 1 shows some typical variations of residential building forms along the street. Four representative variations are considered in this paper, i.e. rotation, stagger, bend and annex building. The rotation, stagger and bend variations of buildings are closely related to the street orientations and the demand for daylighting. Annex buildings are quite common along the street in residential areas for commercial purposes, which are generally parallel to the street for larger commercial space regardless of the street orientations.



Figure 1. a) Street networks and b) residential areas of Nanjing. c) Typical variations of residential building forms along the street.

CFD simulation

Building configurations (Figure 2) are established according to the morphology characteristics analysis. The length and width of each building are 48m and 12m respectively. The height of each building is 18m (H). The width and height of annex building are 6m and 9m respectively. The distance between buildings in NS direction is 24m and in EW direction 8m. Each residential area is $336\text{m} \times 308\text{m}$ ($x \times y$), which makes the street intersection distances closed to the statistical results (300m). The street width is set as 16m. Two representative orientations of the research street are investigated, i.e. NS and EW. All the residential buildings along the streets take a regulated backward distance of 4m away from the street edges. Figure 3 shows the cases of different building form variations and the form parameters.

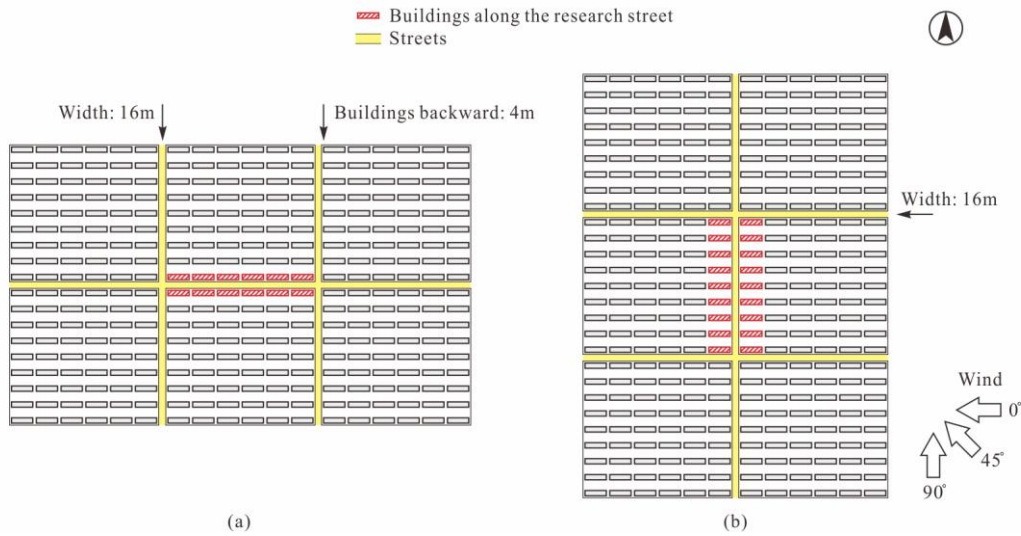


Figure 2. Building configurations of a) EW and b) NS streets.

	Research street in EW orientation	Research street in NS orientation
Rotation	<p>Case R-EW-1: $\theta=0^\circ$ Case R-EW-2: $\theta=12^\circ$ Case R-EW-3: $\theta=24^\circ$</p>	<p>Case R-NS-1: $\theta=90^\circ$ Case R-NS-2: $\theta=78^\circ$ Case R-NS-3: $\theta=66^\circ$ Case R-NS-4: $\theta=0^\circ$</p>
Stagger	<p>Case S-EW-1: $X1/X=0.5, Y1/Y=0.2$ Case S-EW-2: $X1/X=0.5, Y1/Y=0.4$ Case S-EW-3: $X1/X=0.4, Y1/Y=0.4$</p>	<p>Case S-NS-1: $X1/X=0.5, Y1/Y=0.2$ Case S-NS-2: $X1/X=0.5, Y1/Y=0.4$ Case S-NS-3: $X1/X=0.4, Y1/Y=0.4$</p>
Bend	<p>Case B-EW-1: $X1/X2=1, \theta=150^\circ$</p>	<p>Case B-NS-1: $X1/X2=1, \theta=150^\circ$</p>
Annex building	<p>Case A-EW-1: $Y1=0\text{m}$ Case A-EW-2: $Y1=6\text{m}$</p>	<p>Case A-NS-1: $X1=0\text{m}$ Case A-NS-2: $X1=-6\text{m}$</p>

Figure 3. Cases of different building form variations and respective form parameters.

The lateral boundaries of the entire computational domain are set $10H$ away from the buildings, while the height of the computational domain is $6H$. The blockage ratio is less than 3%, as recommended by Tominaga et al. (2008). The hexahedral grids are generated. The grid

resolution meets the major simulation requirements recommended by Tominaga et al. (2008). The grid sensitivity analysis shows the errors caused by grid resolutions have an unnoticeable effect on the numerical results. The inlet profiles presented by Richards and Hoxey (1993) are set as the inflow boundary conditions. Three wind directions 0°, 45° and 90°, shown in Figure 2, are analyzed. The velocity profile (U), the turbulent kinetic energy profile (k) and turbulent dissipation rate profile (ε) are calculated by is calculated by

$$U(z) = \frac{u_{ABL}^*}{\kappa} \ln \left(\frac{z + z_0}{z_0} \right) \quad (1)$$

$$k(z) = \frac{u_{ABL}^{*2}}{\sqrt{C_\mu}} \quad (2)$$

$$\varepsilon(z) = \frac{u_{ABL}^{*3}}{\kappa(z + z_0)} \quad (3)$$

where z is the height coordinate (m), z_0 the aerodynamic roughness length (m), κ the von Karman constant (0.42), u_{ABL}^* the atmospheric boundary layer friction velocity (m/s) and C_μ is a constant (0.09). Zero static gauge pressure condition is defined as the outflow boundary condition. At the top and lateral boundaries, the symmetry boundary conditions are applied. Non-slip wall boundary conditions are specified at the ground surface and all the building surfaces. ANSYS Fluent is applied to solve steady RANS equations for incompressible and isothermal flow. The standard k- ε turbulence model is used to simulate turbulence effects. The SIMPLE algorithm is utilized for pressure-velocity coupling. Pressure interpolation is in second order accuracy. For both the convection terms and the viscous terms of the governing equations, second-order discretization schemes are used.

To simulate the pollutant emission by vehicles, a uniformly distributed passive pollutant source (CO, carbon monoxide) is defined from ground up to pedestrian level (2m) in the streets. The pollutant emission rate (\dot{m} , kg/m³ s) is set to 10⁻⁵kg/m³ s. The concept of purging flow rate (PFR) was introduced to predict the net rate of removing pollutant in urban domain by Bady et al. (2008). The pedestrian purging flow rate (PFR_{ped} , m³/s) is calculated by Eq. (4), where \bar{c} is the local pollutant concentration (kg/m³) and Vol is the pedestrian volume in the research street ($z=0-2m$).

$$PFR_{ped} = \frac{\dot{m} \times Vol}{\int_{Vol} \bar{c} dx dy dz / Vol} \quad (4)$$

3 RESULTS

Impact of wind directions

PFR indicates the net rate of removing pollutant. Thus, higher values of PFR_{ped} indicate better street ventilation. Figure 4 illustrates PFR_{ped} of different cases of 0°, 45° and 90° inflow wind directions. Figure 4 shows that PFR_{ped} is greatly influenced by wind directions. When the wind is parallel to the research street, the pollutants from the upstream streets will accumulate in the research streets. With regard to the EW streets, PFR_{ped} of 0° inflow wind direction are generally lower than PFR_{ped} of 45° and 90° inflow wind directions, owing to the pollutant accumulation from the upstream streets. Besides, in general, pollutant dispersions of 90°

inflow wind direction are better than which of 0° and 45° inflow wind directions. With regard to the NS streets, PFR_{ped} of 90° inflow wind direction are much lower than PFR_{ped} of 0° and 45° inflow wind directions, owing to the pollutant accumulation from the upstream streets. Besides, pollutant dispersions of 45° inflow wind direction are better than which of 0° and 90° inflow wind directions.

Impact of form variations

The impacts of building form variations to PFR_{ped} are different in different inflow directions. With regard to the EW streets, the rotation, stagger and bend variations of the buildings are favorable to pollutant removal under the 0° and 90° inflow wind directions, while annex buildings have unnoticeable effects on improving pollutant removal. However, under the 45° inflow wind direction, the rotation, stagger variations and annex buildings deteriorate pollutant removal. Therefore, in general, the rotation, stagger and bend variations of the buildings are favorable to street ventilation, while annex buildings are not conducive. With regard to the NS streets, the building form variations are unfavorable to pollutant removal under the 0° and 45° inflow wind directions, particularly for annex buildings, while the form variations have unnoticeable effects on pollutant removal under the 90° inflow wind direction. Besides, for both EW and NS streets, the rotation angles (θ) affect the street ventilation significantly. The stagger parameters (X1/X and Y1/Y) and annex building parameters (X1 or Y1) have unnoticeable differences on the street ventilation. Therefore, appropriate building form variations are favourable to street ventilation and pollutant dispersion for EW streets. However, building form variations are not conducive to street ventilation for NS streets. Besides, the annex buildings usually deteriorate the street ventilation.

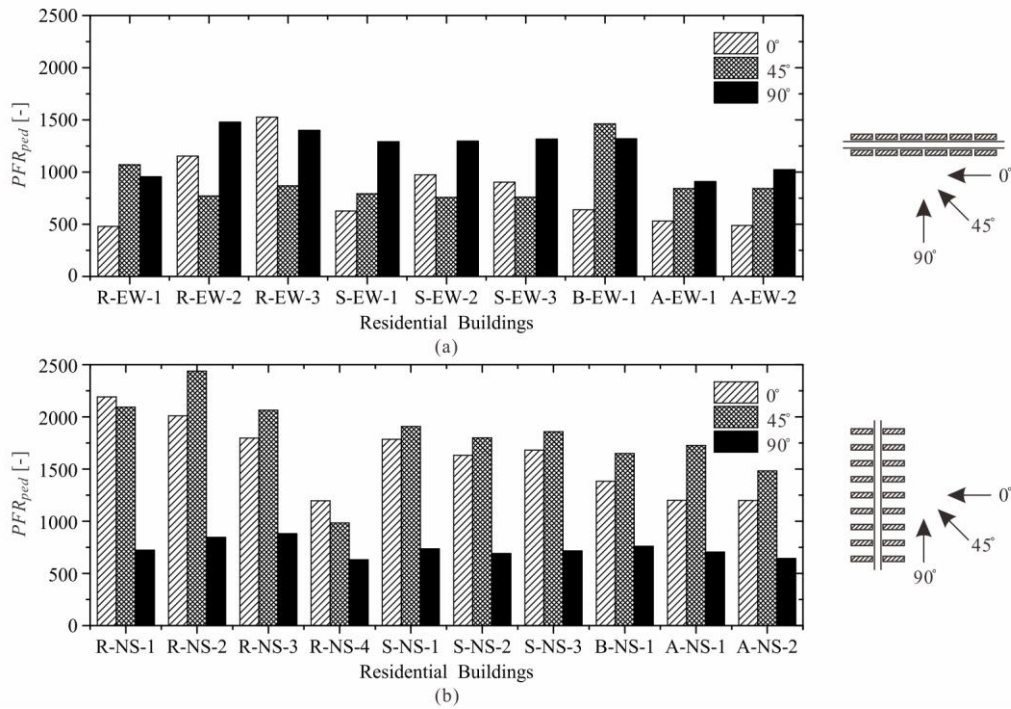


Figure 4. PFR_{ped} of different cases of a) EW streets and b) NS streets.

4 DISCUSSION

Wind directions and building form variations have significant impacts on the pollutant dispersion. Appropriate building form variations are favourable to pollutant dispersion for EW streets, while unfavourable for NS streets. Besides, the annex buildings will deteriorate the pollutant dispersion.

Pollutant dispersion in streets is initially introduced in this paper. In order to better understand the process of pollutant dispersion, pollutant transport rates of mean flow and turbulent diffusion through street roofs and lateral openings will be studied in further investigations.

5 CONCLUSIONS

This paper investigates the influence of four representative residential building form variations to the street pollutant dispersion in the case of Nanjing. According to the quantitative analysis to the streets and residential buildings of Nanjing, the representative street structures, residential buildings and building form variations are present. The numerical results show that wind directions and building form variations have significant impacts on the pollutant dispersion. Appropriate building form variations are favourable to street ventilation and pollutant dispersion for EW streets, while unfavourable for NS streets. Therefore, in order to facilitate the street ventilation, the prevailing wind directions and street orientations of the city should be taken into considerations in urban and building design. Besides, the annex buildings, usually for commercial purposes, will deteriorate the street ventilation.

6 ACKNOWLEDGEMENT

The research was supported financially by the key project of the National Science Foundation of China on “Urban form - microclimate coupling mechanism and control” through Grant No. 51538005.

7 REFERENCES

- Bady M., Kato S., Huang H., 2008. Towards the application of indoor ventilation efficiency indices to evaluate the air quality of urban areas. *Building and Environment*, 43, 1991-2004.
- Di Sabatino S., Buccolieri R., Pulvirenti B., Britter R., 2007. Simulations of pollutant dispersion within idealized urban-type geometries with CFD and integral models. *Atmospheric Environment*, 41, 8316-8329.
- Hang J., Sandberg M., Li Y.G., Claesson L., 2009. Pollutant dispersion in idealized city models with different urban morphologies. *Atmospheric Environment*, 43, 6011-6025.
- Hang J., Li Y.G., Sandberg M., Buccolieri R., Di Sabatino S., 2012. The influence of building height variability on pollutant dispersion and pedestrian ventilation in idealized high-rise urban areas. *Building and Environment*, 56, 346-360.
- Hang J., Wang Q., Chen X.Y., Sandberg M., Zhu W., Buccolieri R., Di Sabatino S., 2015. City breathability in medium density urban-like geometries evaluated through the pollutant transport rate and the net escape velocity. *Building and Environment*, 94, 166-182.
- Hu T., Yoshie R., 2013. Indices to evaluate ventilation efficiency in newly-built urban area at pedestrian level. *Journal of Wind Engineering and Industrial Aerodynamics*, 112, 39-51.
- Lin M., Hang J., Li Y.G., Luo Z.W., Sandberg M., 2014. Quantitative ventilation assessments of idealized urban canopy layers with various urban layouts and the same building packing density. *Building and Environment*, 79, 152-167.
- Ramponi R., Blocken B., de Coo L.B., Janssen W.D., 2015. CFD simulation of outdoor ventilation of generic urban configurations with different urban densities and equal and unequal street widths. *Building and Environment*, 92, 152-166.
- Richards P.J., Hoxey R.P., 1993. Appropriate boundary conditions for computational wind engineering models using the k- ϵ turbulence model. *Journal of Wind Engineering and Industrial Aerodynamics*, 46&47, 145-153.
- Salim S.M., Buccolieri R., Chan A., Di Sabatino S., 2011. Numerical simulation of atmospheric pollutant dispersion in an urban street canyon: Comparison between RANS and LES. *Journal of Wind Engineering and Industrial Aerodynamics*, 99, 103-113.
- Tominaga Y., Mochida A., Yoshie R., Kataoka H., Nozu T., Yoshikawa M., Shirasawa T., 2008. AIJ guidelines for practical applications of CFD to pedestrian wind environment around buildings. *Journal of Wind Engineering and Industrial Aerodynamics*, 96, 1749-1761.